CDF/DOC/PLUG_UPGR/PUBLIC/3195

YIELDS, COMPOSITIONS AND PARTICLE IDENTIFICATION IN THE 1996 CDF TEST-BEAM

M. A. Frautschi, O. Ganel* and R. Wigmans
Department of Physics
Texas Tech University
Box 41051
Lubbock, TX 79409-1051

5 September 1996

Abstract

Results of simulations are used to estimate yields and beam compositions for the 1996 run of Meson Test (MT). These show that minor modifications are expected to increase the rates from 1991 ten-fold and more.

Two options for particle identification are compared: the historical Čerenkov counter and a preshower detector. Based on a comparison of a number of factors, and the relative purity of low momentum electron beams produced from high momentum hadron beams, the preshower detector has emerged as the option of choice.

*Contact: opher@tthep1.phys.ttu.edu

Contents

List of Tables

List of Figures

1 Introduction

This note is intended to summarize the anticipated running conditions for Meson Test (MT), the CDF test-beam, in 1996. This includes yields and beam compositions estimated by simulations, as well as the provisions made for particle identification.

In general, two running modes are expected. The first is the hadron beam mode. In this mode, a primary target in M02 will be placed in the beam. Secondaries coming from interactions in the target with the appropriate momentum and angles will form the beam, which will be transported down to MT6. Hadron beam momentum will be determined by the location of the primary target within the string of bending magnets where MT is extracted from the primary beam (MW2WD2).

There are three wheel targets (MT2CON1, MT2CON2 and MT2CON3). Each target is located upstream of one or more of the MW2WD2 bending magnets. MT2CON1 is positioned upstream of all three magnets, allowing 227 GeV/c secondaries to be swept into the acceptance of MT. MT2CON2 is positioned between MW2WD2-1 and MW2WD2-2, which will allow MW2WD2-2 and MW2WD2-3 to bend 150 GeV/c secondaries into MT. MT2CON3 is positioned between MW2WD2-2 and MW2WD2-3, which will allow MW2WD2-3 to bend 75 GeV/c secondaries into MT.

A fourth target (MT2CON4) is positioned on a track going through MW2WD2-3. The position of MT2CON4 in the magnet determines the total bending power exerted on the secondaries ($\int \mathbf{B} \cdot \mathbf{dl}$). This in turn determines the mean momentum of the particles reaching the next aperture in MT.

The second running mode will be used for positron beams. Here, a 150 GeV/c or 227 GeV/c secondary beam will be transported to a radiator (MT3CON1). This beam will be a hadron beam with a small fraction of positrons. At MT3CON1 this beam will impinge on a radiator of at most 0.1 λ_{int}. More than 90% of the hadrons will go through the radiator unaffected and will not be transported through the remainder of the beamline which will be tuned for lower momenta. The high momentum positrons will go through the radiator and radiate energy away in the form of bremsstrahlung photons. These photons will mostly convert into electron-positron pairs. Out the back of the radiator will come positrons with a wide spectrum of momenta, peaked at low values (photons and negative electrons will not be picked up by the beamline). Most low-momentum tertiary hadrons coming from the 10% (or less) of secondary hadrons that will interact in the radiator, will have too high or too low momentum values, too large an angle to the beam axis, or both, and will thus not be accepted and transported to MT6. A large fraction of the low momentum pions that do get picked up will decay in-flight. Tertiary positron production from secondary hadrons interacting in the radiator is expected to provide a negligible contribution to positron yield in this mode. The resulting low-momentum positron beam is expected to be very pure.

The note is arranged as follows. Section 2 lists the assumptions made in the simulations. Section 3 compares simulations of 1987-1991 runs with actual results to validate the simulations. Section 4 lists planned changes and how they are expected to impact yields. Sections 5 and 6 summarize the yields and purity of hadron and positron beams, respectively, expected in 1996. Section 7 discusses particle identification. Section 8 makes some suggestions that may improve MT. The conclusions are listed in section 9. Detailed yield calculations for hadrons and positrons are given in appendices A and B, respectively. Appendix C provides a list of parameters for the Čerenkov counter.

2 Simulation Assumptions

Any simulation is based on assumptions. Many of these are implicit in the choice of simulation software package. Others are explicitly made in setting parameters or switches, or in deciding what values to use in variables that go into calculations.

The simulation packages used were DECAY-TURTLE [1] as modified by A. Malensek [2] for both hadrons and positrons. EGS4 [3] was used to simulate the interaction of positrons with the radiator (MT3CON1). Optimization of quadrupole field strengths was done using TRANSPORT [4].

The explicit assumptions made in the simulations reported here are as follows:

- The trigger is determined by a 1"×1" area in MT6. There will be significant yields outside this trigger area which may be used, but this provides a useful benchmark.
- For positron production, the secondary beam spot on MT3CON1 is assumed to be 3"×3".
- The momentum bin-width for positrons exiting MT3CON1 which is of interest has a 8% half-width (e.g. 50 GeV/c $\pm$ 4 GeV/c). This is used in both the EGS and the DECAY-TURTLE simulations, and thus does not affect the yield (the only requirement is that this width is larger than the MT3CON1-MT6 momentum acceptance width).

Assumptions made in calculations are as follows:

- The primary beam intensity is assumed to be 1.0×10^{12} primary protons for each 20 second spill. This may turn out to be optimistic, in which case particle rates would go down.
- The primary target thickness in 1996 will be 0.184 λ_{int} such that the fraction of primary protons expected to interact in the primary target in 1996 will be 0.168 (based on $\mathrm{N_{interacting}(z)/N_0 = 1.0 - e^{-z/\lambda_{int}}}$).

Some important modifications were made in the simulation input decks with respect to those used previously:

- The Z positions of all the beam elements have been corrected based on tape-measure measurements made by O. Ganel and R. Tokarek in January '96. The most notable correction is that the distance between MT4Q1 and MT4Q2 (see figure 1) has been changed from 12 feet to 21 feet. Following these corrections a better optimization of quadrupole currents became possible which led to simulations of the MT beamline showing an increased yield for hadron beams over simulations of the previous run.
- DECAY scales all magnet currents by a factor of $\mathrm{P_0/P_{ref}}$ (for MT, $\mathrm{P_{ref}}$ = 245 GeV/c). This is needed for MT magnets. The MW magnets around the primary MT targets, however, are set for 800 GeV/c primary protons. Their currents should thus be set higher by a factor of $\mathrm{P_{ref}/P_0}$ to offset the scaling. The momentum selection of secondaries here is executed by using different targets (MT2CON1 for 227 GeV/c beams, MT2CON2 for 150 GeV/c, MT2CON3 for 75 GeV/c and MT2CON4 crawler inside MW2WD3 bending magnet for momenta lower than 75 GeV/c - see figure 1).
- For $\mathrm{P_{secondary}} <$ 75 GeV/c the length of MW2WD3 has been decreased linearly with momentum to reflect the position of the crawling target.
- All input decks have been translated to the MAD [5] format.

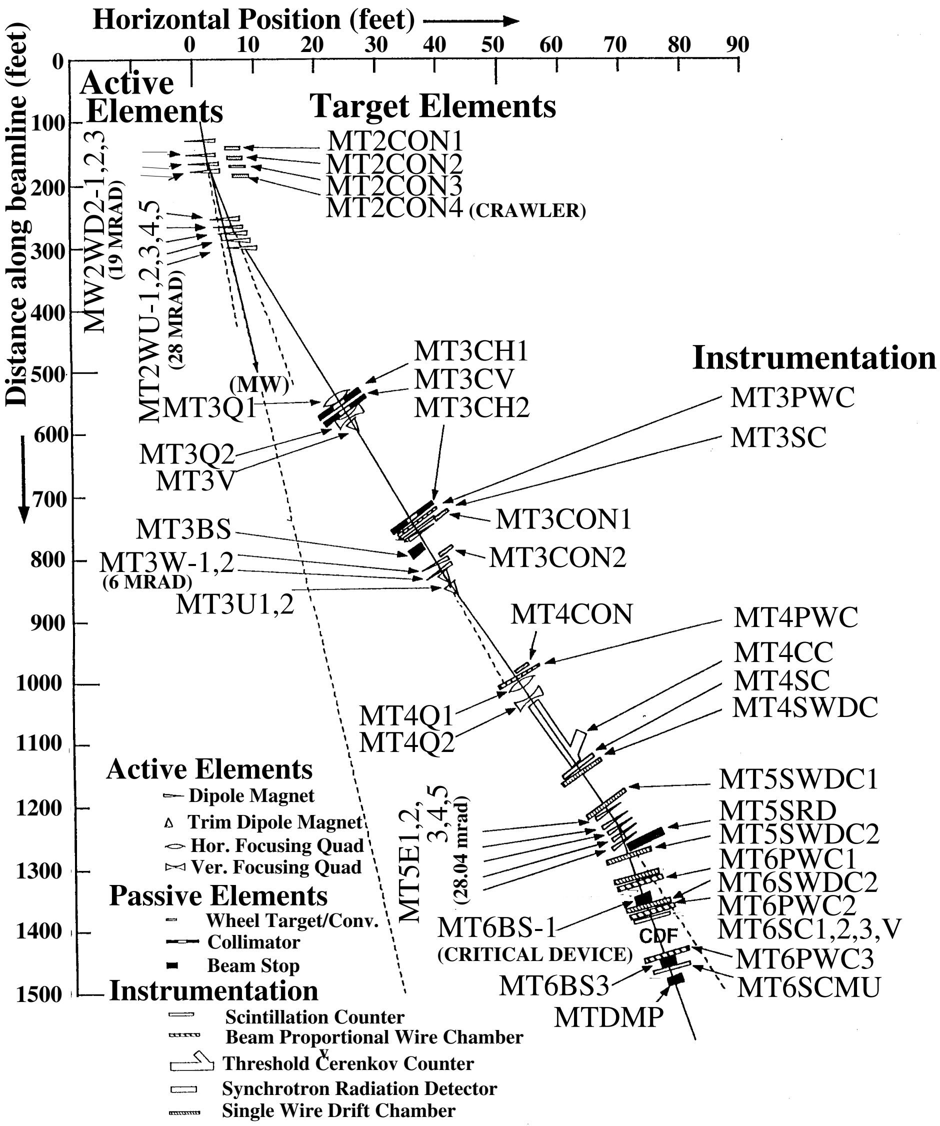

Figure 1: Meson Test (MT) beamline

3 Comparing Simulation to Experimental Data

To compare the results obtained by simulations to actual data, the conditions in previous runs (1991) were simulated. The magnet settings and actual yields were extracted from log-books. The yields were listed in terms of the ratio MTSC46/MW1SEM. This is probably a coincidence of MT4SC (a 2”×2” scintillator) with a combination of scintillators in MT6 (which have a 1”×1” common area), divided by the number of primary protons seen in the Meson West (MW) beamline, in M01, upstream of MT.

3.1 Comparison of Hadron Beams

Simulated yields were obtained separately for π's and protons. These were summed and adjusted for the expected fraction of positrons and muons in the beam. The November 1987 yields were adjusted by a factor of 0.9529 to account for the 8.9 $\lambda_{\rm int}$ (8.5%) target used then as opposed to the 8.4 $\lambda_{\rm int}$ (8.1%) target used in 1990-91 as well as in the simulations. Comparing the simulated yields to the experimentally observed yields (see figure 2 and table 1), one finds the simulation over-estimating the November 1987 values by factors up to 4.1 and under-estimating the 1990-91 data by factors up to 2.6 which puts the simulation in the same order of magnitude as both data-sets, and bracketed by them.

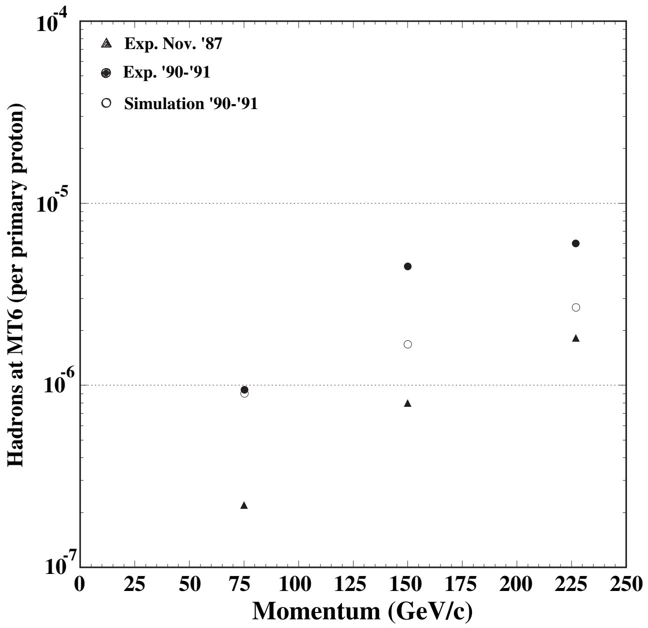

Figure 2: Hadron yields in 1987-1991 runs vs. simulated 1991 yields

Momentum	Yield at MT6 ($\times 10^6$ particles/spill)		
(GeV/c)	Nov. 1987	1990-91	Simulated 1990-91
75	0.22	0.95	0.90
150	0.80	4.50	1.71
227	1.82	6.00	2.74

Table 1: Hadron beam yields from simulations and data

It is unclear what caused the data to increase by factors of 4.3, 5.6 and 3.3 respectively, from 1987 to 1991. It is possible that the beam was better tuned in the latter run, or that external conditions (e.g. interference from magnets of other beamlines upstream of the MW-MT split that cause the beam to be shifted slightly) lessened between the two time periods, or that collimator settings differed between the two runs.

3.2 Comparison of Positron Beams

The only setting information found on positron tunes in the log-books is for the 1990 run. Unfortunately, the only positron yield information (including particle identification) is from November of 1987. Assuming the 1990 yield curve was similar to the November 1987 one, a comparison of simulation and data is possible. The yields from simulation of the 1990 settings are adjusted by the ratio of measured hadron beam yields for 1990 conditions and measured yields in 1987, for the 227 GeV/c beam used for positron production (see figure 3 and table 2).

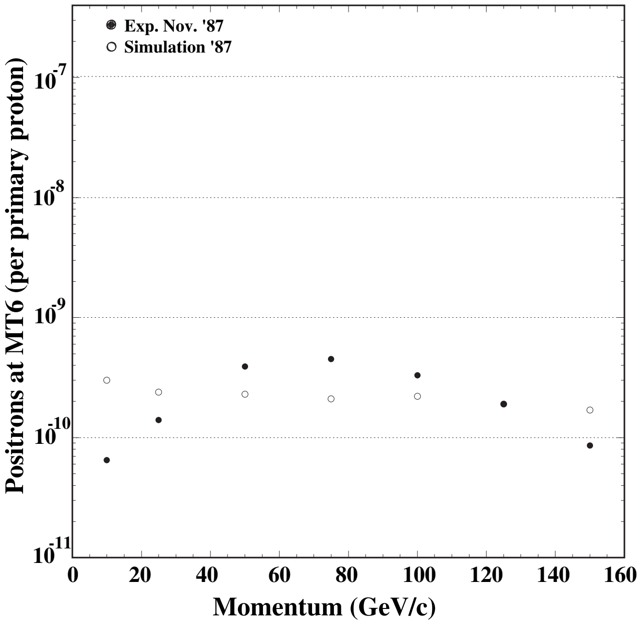

Figure 3: Positron yields in 1987 run vs. simulated 1987 yields

Momentum	Yield at MT6 (e^+/spill)	
(GeV/c)	Nov. 1987 data	Simulated 1987 conditions
10	65	300
25	140	240
50	390	230
75	450	210
100	330	220
125	190	190
150	86	170

Table 2: Positron yields from simulations and data

As can be seen from the figure as well as from the table, the simulation of the 1987 yield is in the same order of magnitude as the data from Nov. 1987. The differences could be explained by a combination of the following effects (which were not simulated):

- High energy positrons suffer greater synchrotron losses in the MT5E bending string compared to low energy positrons. This could explain the discrepancy between simulation and data at the high-momentum end.

- Multiple scattering effects, especially in the Čerenkov counter, affect the path of low-energy positrons more than that of high-energy particles. This effect could explain the discrepancy between simulation and data at the low-momentum end.

4 Modifications in the 1996 MT Beam

Simulations indicate that it should be possible to increase the yield of MT by at least a factor of 10, without costly modifications such as additional quadrupole magnets.

- An overall increase in yields can be achieved by increasing the thickness of the primary targets (MT2CON1, MT2CON2, MT2CON3 and MT2CON4) so that 16.8% of primary protons will interact in the target. This was not possible in previous runs as MT was running parasitically off MW which had higher priority users.
- Simulations suggest that the quadrupole current settings were not optimal in the 1987-1991 runs. Tables 3 and 4 show the optimal settings for a 227 GeV/c hadron beam and a 50 GeV/c positron beam. The suggested settings can be seen to be out of the ranges used in tuning the beam in the previous runs (the conversion between currents and pole field strengths uses an approximately linear relation with a slope of 0.052 kG/inch/A up to 80 A, and curves lying somewhat below that line beyond 80 A). The change in settings may afford an increase of up to a factor of 2 compared to previous runs.

Quadrupole	I_{min} (A)	B_{min} (kG)	I_{set} (A)	B_{set} (kG)	I_{max} (A)	B_{max} (kG)	$\mathbf{I_{1996}}$ **(A)**	$\mathbf{B_{1996}}$ **(kG)**
MT3Q1	50	3.90	79	6.16	90	6.54	**45**	**3.52**
MT3Q2	64	4.99	84	6.31	94	6.81	**48**	**3.75**
MT4Q1	48	3.74	55	4.29	85	6.39	**43**	**3.37**
MT4Q2	40	3.12	55	4.29	80	6.24	**40**	**3.09**

Table 3: 227 GeV/c π^+ Tune

Quadrupole	I_{min} (A)	B_{min} (kG)	I_{set} (A)	B_{set} (kG)	I_{max} (A)	B_{max} (kG)	$\mathbf{I_{1996}}$ **(A)**	$\mathbf{B_{1996}}$ **(kG)**
MT3Q1	76	5.93	81	6.25	94	6.81	**30**	**3.52**
MT3Q2	76	5.93	84	6.31	94	6.81	**32**	**3.75**
MT4Q1	18	1.40	18	1.40	26	2.03	**9.5**	**0.741**
MT4Q2	18	1.40	21	1.64	26	2.03	**8.7**	**0.679**

Table 4: 50 GeV/c e^+ Tune

- An increase in the positron yield can be achieved by the following changes:
  - Using the 150 GeV/c beam instead of the 227 GeV/c beam to provide more than twice as many high-momentum positrons incident on the radiator (MT3CON1).

– Matching the radiator thickness to the desired final positron momentum. This matching is expected to increase rates by as much as a factor of 2.5 for low and high momentum positrons. For momenta in the 25-75 GeV/c range this will not have a large effect.

5 Hadron Beams in 1996

Incorporating the suggested changes to the simulations, the expected hadron beam yields for 1996 were calculated (see figure 4 and table 5 for the results, and Appendix A for details of the calculation used).

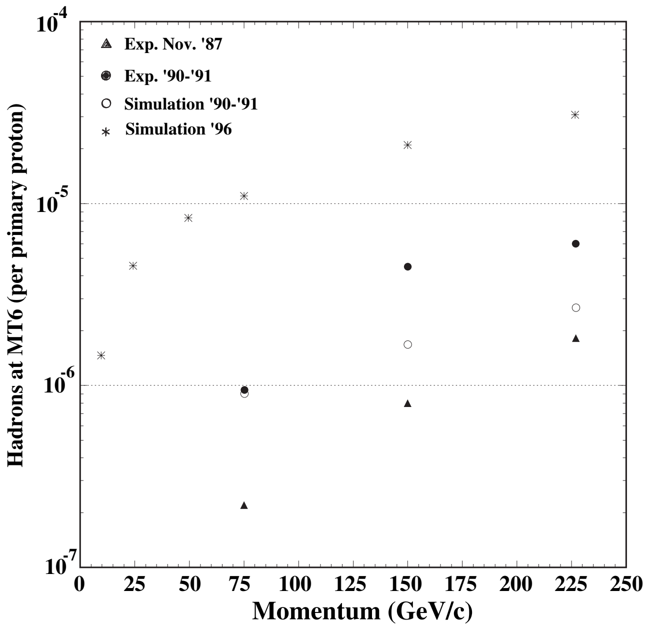

Figure 4: Hadron yields in 1987-1991 vs. simulated 1991 and 1996 yields

p (GeV/c)	Yield at MT6 ($\times 10^6$ particles/spill) π^+	p	e^+	μ^+	total
5	0.046	4×10^{-3}	0.49	0.01	0.54
10	0.32	0.017	1.0	0.05	1.3
25	1.9	0.11	2.2	0.23	4.4
50	4.8	0.43	3.1	0.35	8.7
75	6.8	0.97	2.6	0.26	11.
150	14.	4.7	1.5	0.38	21.
227	18.	12.	0.72	0.23	31.

Table 5: Hadron Beam Yields for π's, Protons, Positrons and μ's

At lower momenta, the proton production cross-section is even lower than at 5 GeV/c, and the pion survival fraction is less than that at 5 GeV/c. Accordingly, producing a secondary beam of (e.g.) 1 GeV/c hadrons is not foreseen to be practical.

Producing low momentum tertiary hadrons in MT is excluded. At 5 GeV/c, under optimistic assumptions, where 150 GeV/c hadrons hit a 1.0 λ_{int} target at MT4CON1 (immediately upstream of the MT4 quadrupole magnets), the hadron yield will be approximately 1.2×10^{-12} hadrons at MT6 per primary proton, providing (on average) 1.2 hadrons per spill at MT6. At momenta below 5 GeV/c the yield will be even lower. Hitting MT4CON1 with a 75 GeV/c hadron beam will cause the yield to drop by a factor of 4. Using the 227 GeV/c beam would afford an increase of less than factor 2.

From table 5 it is easy to calculate the expected beam composition of hadron beams at various momenta (see figure 5 and table 6).

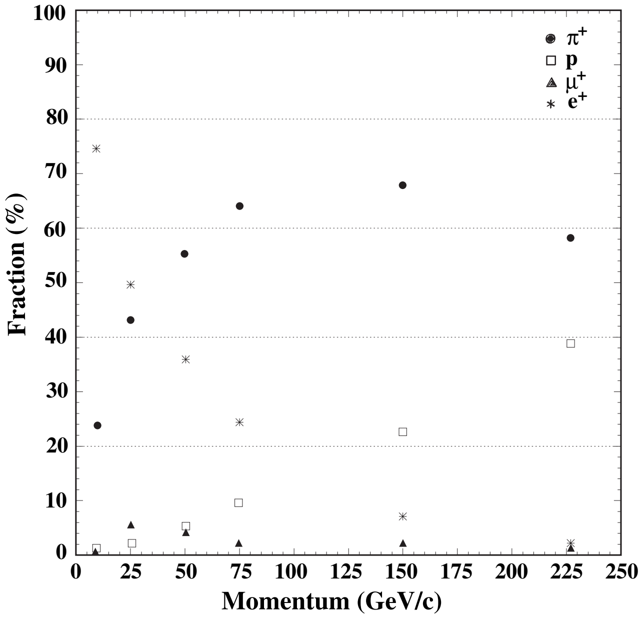

Figure 5: Simulated hadron beam compositions in 1996

p (GeV/c)	π^+	p	e^+	μ^+
5	0.085	0.007	0.906	0.002
10	0.238	0.013	0.745	0.004
25	0.428	0.025	0.495	0.052
50	0.553	0.050	0.357	0.040
75	0.640	0.091	0.245	0.024
150	0.680	0.228	0.073	0.019
227	0.582	0.388	0.023	0.007

Table 6: Hadron Beam Compositions

During the previous run, hadron beam composition at 227 GeV/c was measured to be 0.985±0.002 π^+/p, 0.008±0.001 μ^+, 0.007±0.001 e^+.

6 Positron Beams in 1996

Incorporating the suggested changes to the simulations, the expected positron beam yields for 1996 were calculated (see figure 6 and table 7 for the results, and Appendix B for details of the calculation used - note that all three columns are simulation results). Note that since the Pb radiator thickness is matched to desired positron momentum, the shape of the curve in figure 6 does not reflect the shape that would be obtained with a single radiator, and the high and low momentum yields are increased with respect to the constant thickness (1.5 X_0) case.

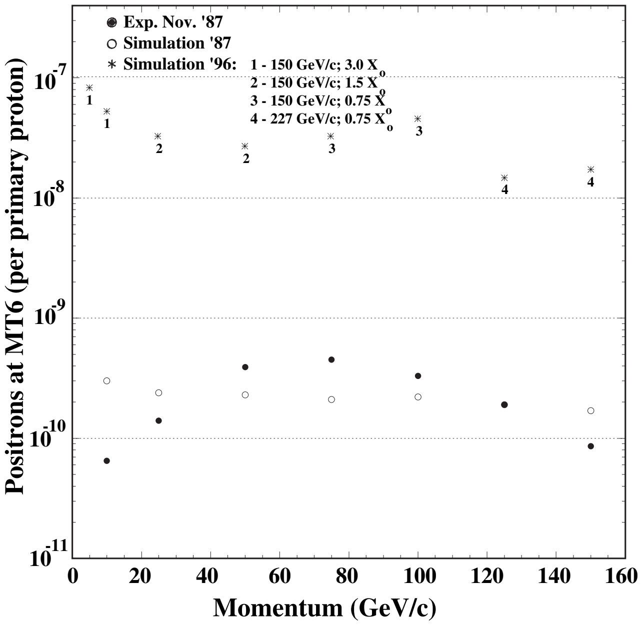

Figure 6: Positron yields in 1987 vs. simulated 1996 yields

Momentum (GeV/c)	Simulated yield at MT6 (e^+/spill)		
	1989 (227 GeV/c; 1.36 X_0)	1996 (150 GeV/c; 1.50 X_0)	1996
1	49	6300	17000 (150 GeV/c, 3.00X_0)
5	330	46000	82000 (150 GeV/c, 3.00X_0)
10	300	38000	51000 (150 GeV/c, 3.00X_0)
25	240	32000	32000 (150 GeV/c, 1.50X_0)
50	230	25000	25000 (150 GeV/c, 1.50X_0)
75	210	23000	31000 (150 GeV/c, 0.75X_0)
100	220	16000	42000 (150 GeV/c, 0.75X_0)
125	190	9000	15000 (227 GeV/c, 0.75X_0)
150	170	6800	17000 (227 GeV/c, 0.75X_0)

Table 7: Positron yields from simulation of various conditions

Note that the rather slow decline in positron yield with rising momentum results in large part from the growing bin widths (e.g. 150 GeV/c ± 12 GeV/c compared to 5 GeV/c ± 0.4 GeV/c).

The production of low-momentum *hadrons* in the radiators will occur at most for 10% of secondary hadrons reaching MT3CON1 (radiator thickness will be at most $3X_0 \sim 0.1\lambda_{int}$). The tertiary hadrons produced in this process will have a much broader angular distribution than the positrons (on average, these hadrons acquire a transverse momentum of 0.3 GeV/c with respect to the direction of the incident hadron). The limited momentum acceptance of the MT3-MT6 portion of the beamline will also limit hadron contamination of the low-momentum positron beams. Finally, at low momenta especially, many pions will decay in-flight before reaching MT6.

When putting all these factors together we find that the predicted hadron contamination of the positron beams is small. At the lowest momenta we'd expect at most a few hadrons per spill, and at the highest momenta (e.g. 150 GeV/c) we'd expect less than 100 hadrons per spill. The positron beams should thus be more than $> 95\%$ pure (see table 8).

Momentum	Yield at MT6 (particles/spill)	
(GeV/c)	e^+	hadrons
1	17000 (99.99%)	1 (0.01%)
5	82000 (100.0%)	1 (0.00%)
10	51000 (99.99%)	7 (0.01%)
25	32000 (99.97%)	9 (0.03%)
50	25000 (99.93%)	19 (0.07%)
75	31000 (99.97%)	9 (0.03%)
100	42000 (99.98%)	7 (0.02%)
125	15000 (99.70%)	45 (0.30%)
150	17000 (99.81%)	32 (0.19%)

Table 8: Hadron contamination of positron beams in 1996 (simulation)

7 Particle Identification in MT

At high momenta, the natural fraction of π's and protons produced in hadronic interactions is much greater than that of positrons. At low momenta, positrons are produced copiously, but hadrons and muons (from pion decay) still comprise a large fraction of shower particles. Production of pure positron beams thus presents a serious challenge. This challenge can be met, however, by careful design of the positron beam production method.

The production of positron beams in MT, in 1996 is designed in such a way that they are expected to be very pure. This will be achieved by:

- Choice of secondary beam momentum incident on a radiator (MT3CON1).
- Target thickness and (high-Z) material.
- Target position with respect to the detector.
- Aperture of MT5E bending string.

In previous runs identification of positrons was based in large part on a Čerenkov counter. For the upcoming run in late 1996, this identification method has been reviewed and compared to preshower detector based particle identification.

- The pions that are produced will have a p_T of approximately 0.3 GeV/c on average. This corresponds to a production angle of 30 mr. A substantial fraction of these pions will miss the aperture of the bending magnets downstream.
- A substantial fraction of the transmitted pions will decay in flight:

$$\begin{array}{lcr} \text{Energy} & \approx & 10 \text{ GeV} \\ \gamma \times \beta & = & 71.4 \\ c \times \tau \text{ for } \pi^{\pm} & = & 7.804 \text{ m} \\ \gamma \times \beta \times c \times \tau & = & 557 \text{ m} \\ \text{distance from Čerenkov counter to M06} & \approx & 72 \text{ m} \\ & & \\ \text{fraction surviving in} - \text{flight decays} & = & \exp(-72 \text{ m}/557 \text{ m}) \times 100\% \\ & = & 88\% \end{array} \tag{1}$$

Thus, without benefit of a Čerenkov counter or other particle identification, the beam delivered to M06 will be mostly electrons, with a muon component that can be vetoed using scintillator paddles (MT6SCMU1 and MT6SCMU2), downstream of the existing FHA test module (15 λ_{int}).

It is appropriate to consider the benefits of retaining the present Čerenkov counter for the 1996 run. To this end a cost versus benefits analysis of using the MT4 Čerenkov counter (MT4CC), versus a preshower detector in the 1996 test-beam run is included below.

7.1 Čerenkov Counter Drawbacks

- Increases losses due to multiple scattering, especially for low energy positrons (the Čerenkov counter length is approximately 30 m, providing about $0.1X_0$).

  from PDG booklet, June 1994 edition:

$$\theta_0 = \frac{13.6 \text{ MeV}}{\beta c p} \; z \sqrt{\frac{x}{X_0}} \left[1 + 0.038 \ln \left\{ \frac{x}{X_0} \right\} \right] \tag{2}$$

  where

$$\begin{array}{lcllcl} \theta_0 & = & \text{plane RMS scattering angle} & & & \\ \beta \times c & = & \text{incident particle velocity} & & \approx & c \\ z & = & \text{incident particle charge} & & = & 1 \\ p & = & \text{incident particle momentum (MeV/c)} & & = & 10,000 \text{ MeV/c} \\ x & = & \text{thickness of scatterer} & & \approx & 30 \text{ m for MT4CC Čerenkov} \\ X_0 & = & \text{radiation length of scatterer} & & = & 304 \text{ m for air at STP} \end{array} \tag{3}$$

  thus,

$$\theta_0 = 3.9 \times 10^{-4} \text{ radians} \tag{4}$$

The distance from the end of the Čerenkov counter to the first magnet in the MT5E string (MT5E-1 through MT5E-5) is approximately 15 m. The multiple scattering will thus produce an RMS deflection of:

$$d = 15 \text{ m} \times 3.9 \times 10^{-4} \text{rad} = 5.8 \text{ mm} \tag{5}$$

The average lateral displacement upon exiting the Čerenkov counter is given by:

$$\begin{aligned} y &= \sqrt{1/3} \times \mathrm{d} \times \theta_0 \\ &= \sqrt{1/3} \times 30\mathrm{m} \times 3.9 \times 10^{-4} \text{ radians} \\ &= 6.7 \text{ mm} \end{aligned} \tag{6}$$

To assess how the above lateral and angular shifts from the beamline will affect the transmission of positrons to MT6 a simple DECAY simulation was carried out. In this simulation the particles coming out of the Čerenkov counter had an additional smearing of 6.7 mm σ in both x and y, and of 3.9×10^{-4} radians sigma in both $x - z$ and $y - z$ angles. The result is that about 45% of particles that would have been successfully transported to a 3”×3” area centered on the beam axis at the downstream end of the CDF area are lost.

Based on this simulation, we might expect the rates to double at best if we replaced the Čerenkov counter with an evacuated tube (or replaced its windows with vacuum bearing windows and added a vacuum system).

- The Čerenkov counter has a gas system and supply, pressure regulator, PMT and electronics that must be brought online and maintained. This could require a substantial fraction of a physicist FTE (Full Time Equivalent) during both the setup and the run.
- About one eighth of π’s will decay in-flight between the Čerenkov counter and the End Plug calorimeter.
- The Čerenkov counter material (0.04 λ_{int}) will be a source of additional low-momentum π’s, contaminating low-momentum positron beams.

7.2 Čerenkov Counter Benefits

- Provides an additional electron ID to check End Plug calorimeter’s Preshower detector.
- Can provide trigger.
- Already exists, has some history.

7.3 Preshower Detector Drawbacks

- Reduces mean of, and increases fluctuations in, calorimeter energy deposit. These effects were measured by the SPACAL collaboration for a 1.7 X_0 thick preshower detector used in combination with their calorimeter [6]. Some of their results are given in table 9.

$E_{electron}$ [GeV]	Δ E_{PSD} [GeV]	Δ E/E [%]	σ/E no PSD [%]	σ/E with PSD [%]
5.0	0.236±0.024	4.72±0.47	7.04±0.20	6.92±0.20
9.7	0.298±0.030	3.07±0.31	5.49±0.08	5.29±0.07
20.0	0.166±0.017	0.83±0.08	4.06±0.08	3.99±0.08
40.0	0.221±0.022	0.55±0.06	3.29±0.05	3.24±0.05
80.0	0.274±0.027	0.34±0.03	2.72±0.04	2.71±0.04
150.0	0.296±0.030	0.20±0.02	2.23±0.05	2.28±0.05

Table 9: The average energy deposited in the 1.7 X_0 preshower detector (PSD) of the SPACAL calorimeter given in GeV (column 2) and as a fraction of the incoming electrons' energy (column 3). Columns 4 and 5 give the effect of the PSD on the energy resolution measured with the calorimeter. Column 4 lists the measured energy resolutions ignoring the PSD signals. In column 5, the resolutions obtained combining the PSD and SPACAL signals event-by-event are given.

7.4 Preshower Detector Benefits

- Little or no maintenance.
- Can provide trigger.
- Simple to build and debug.
- Since it will be mounted directly upstream of the End Plug calorimeter, π's will not have the opportunity to decay between the PSD and the calorimeter.
- A simple threshold cut selects pions (below threshold) or electrons (above threshold) with adjustable $e^\pm/\pi^\pm$ separation and electron efficiency: From a paper on Scintillating Fiber calorimetry in which a similar arrangement[1] is described [7] we can estimate the expected benefits of such a setup (see figure 7, table 10).
  - The pion rejection is better than 10:1 for the cut used by these authors (signal 6.7 times higher than that of a minimum ionizing particle), independent of the energy of the minimum ionizing particles, as expected.
  - Since electromagnetic shower profiles are almost energy independent, the energy fraction deposited in the first 2 X_0, and thus the number of shower particles produced in this section, is proportional to the shower energy.

    The number of shower particles observed in the PSD for a given electron energy is broadly distributed, with a most probable value far above the 6.7 minI cutoff value used by the SPACAL collaboration for the energies listed in table 10.

    The (small) fraction of this distribution cut off in this way (the electron inefficiency) is observed to be practically inversely proportional to the electron energy: 0.8±0.2% at 150 GeV, 2.2±0.3% at 80 GeV and 3.1±0.4% at 40 GeV. Such a trend is expected when the signal distribution (the number of shower particles) rises linearly towards a most probable value. Assuming this trend

[1]The PSD had an absorber composed of 5.3 mm tungsten (1.5 X_0, 0.055 λ_{int}) and 0.5 mm lead (0.5 X_0, 0.016 λ_{int}), followed by a 10 mm thick, 15×15 cm^2 scintillation counter.

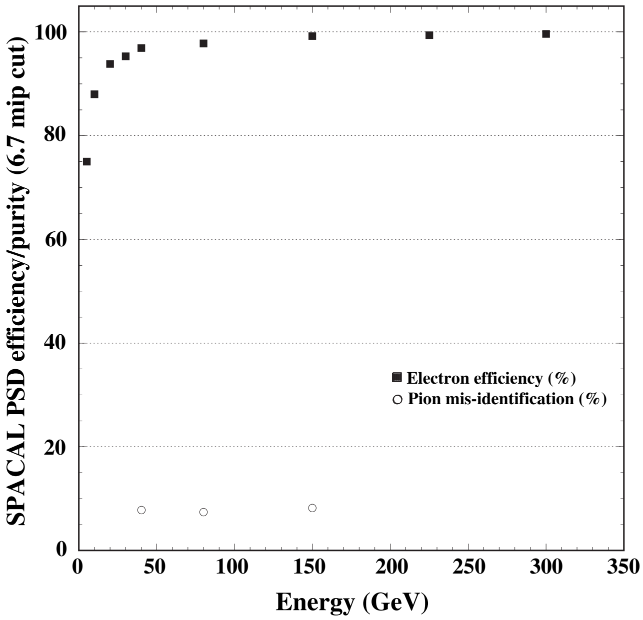

Figure 7: SPACAL PSD e/π separation with 1.7 X_0

continues for lower incident energies, we can estimate the electron inefficiency (and thus the electron efficiency) as in table 10.

We plan to optimize these and other purity/yield issues with the proposed PSD during the commissioning stage of the test-beam.

E [GeV]	π - pass [%]	e^- efficiency [%]
5.0		75±3.2
10.0		88±1.6
20.0		93.8±0.8
30.0		95.3±0.6
40.0	7.8 ± 0.7	96.9±0.4
80.0	7.4 ± 0.6	97.8±0.3
150.0	8.2 ± 0.7	99.2±0.2
225.0		99.4±0.15
300.0		99.6±0.1

Table 10: Fraction of pions passing electron selection cuts and electron efficiencies obtained with a 6.7 min-I cut on the preshower detector pulse height (values below 40 GeV and above 150 GeV are extrapolated).

7.5 Final Choice of Particle Identification Scheme

Based on the cost/benefit analysis above, it was decided to convert the Čerenkov counter to a vacuum pipe by removing the HV and gas, pumping the counter down to vacuum, replacing the upstream window with a thinner window, connecting the downstream end to an adjacent beam-pipe section and removing the parabolic mirror.

Particle identification will be achieved through the use of a preshower detector mounted as part of the End Plug calorimeter module, possibly adding some Pb absorber to augment the steel structural member which now serves as absorber. An additional Preshower detector will be mounted independently and upstream of the End Plug calorimeter. This Preshower calorimeter will be composed of a 2.0 X_0 Pb absorber and a 1 cm thick scintillator paddle, read out by a PMT and will mainly serve for diagnostic purposes during setup.

8 Possible Improvements for MT

Aside from the very obvious comment that 'seeing is believing' and thus one would want to first see *any* particles come out at MT6 before embarking on any complicated, time consuming and/or costly improvements, there is something which should be considered.

During the 1987-1991 runs, for some tunes, a sweeper magnet (MT3SW) had to be turned on to achieve a usable rate. This hints at a misalignment between different segments of the beam. It may thus be useful to tie all the segments of the beamline (i.e. MT2, MT3 part 1, MT3 part 2, MT4-MT5) to a common coordinate system and assess how well they are aligned with each other.

It has been unofficially estimated that this task would take a survey crew 40 hours. With the test-beams at the bottom of the list of priorities, and with the main injector project picking up steam, it will not be easy to obtain that much survey crew time. Such a request has been made of the SAG group.

Another improvement that has been requested, and carried out, is the addition of vacuum pipe from the current downstream end of vacuum pipe (upstream end of MT6) to the furthest downstream point possible (upstream end of MT6BS1).

9 Conclusions

As far as simulations can be trusted, this one predicts that the rates for hadron beams of momenta 5 - 227 GeV/c will be quite considerable - in the range of 46,000 - 30,000,000 particles/spill, and that positron rates will be respectable - in the range of 12000 - 60000 particles/spill (assuming 1.0×10^{12} primary protons per spill).

Below 5 GeV/c there will not be any usable hadron yields.

The above is achievable with relatively simple and inexpensive modifications such as thicker primary targets, matched radiator thicknesses and lower currents in the four quadrupole magnets.

An important consideration, which will limit high momentum hadron rates considerably, is radiation safety. The maximal allowed rates will likely be a few kHz for 227 GeV/c hadrons with a 1×1 inch^2 trigger [8].

10 Acknowledgements

We wish to thank Roger Tokarek, Anthony Malensek and Dan Crane for all their help in getting MT set up again, including but not limited to teaching one of us (O.G.) how to run DECAY and TRANSPORT.

We also wish to thank Yasuo Fukui for his diligent archeological efforts in unearthing information from the logbooks of the previous MT run. His efforts have often been the only source of feedback for how far off reality our results were.

References

[1] *DECAY TURTLE (Trace Unlimited Rays Through Lumped Elements)*
D.C. Carey, K.L. Brown & Ch. Iselin
Fermilab Computing Department report PM-31 or SLAC-246 UC-28 (I/A) (1982).

[2] Private versions of DECAY TURTLE modified by A. Malensek: DECAY.EXE;18 for hadrons and DCYELEC.EXE for electrons.

[3] *Electron Gamma Shower*
W.R. Nelson, H. Hirayama and D.W.O. Rogers
SLAC-Report-165 (1985).

[4] *Third Order Transport, a Computer Program for Designing Charged Particle Beam Transport Systems*
D.C. Carey, K.L. Brown & F. Rothacker
SLAC-R-95-462 (1985).

[5] *The MAD Program (Methodical Accelerator Design)*
H. Grote & F.C. Iselin
CERN/SL/90-13(AP) (1990).

[6] *Electron, Pion and Multiparticle Detection with a Lead/Scintillating Fiber Calorimeter*
D. Acosta *et al.*
Nucl. Instr. and Meth. **A**308 (1991) pp. 481-508.

[7] *Electron-Pion Discrimination with a Scintillating Fiber Calorimeter*
D. Acosta *et al.*
Nucl. Instr. and Meth. **A**302 (1991) pp. 36-46.

[8] *Meson Test Enclosure MT6 Radiation Safety Discussion and Action Items*
M. A. Frautschi and O. Ganel
CDF note CDF/DOC/SAFETY/PUBLIC/3820.

A Hadron Beam Yield Calculations

Private versions of the DECAY-TURTLE executable as modified by Anthony Malensek of Research Division [2] provide the ratio of secondaries produced to interacting incident primaries. This ratio was multiplied by the number of interacting primary protons - 1.68×10^{11} (the assumed primary intensity of 1.0×10^{12} primary protons/spill, multiplied by the target interaction fraction of 0.168) to provide the number of secondaries exiting the primary target. To find the absolute yield, one now needs to multiply the above number by the fraction of secondaries reaching the desired downstream point that lie within the transverse area defined by a trigger. To find this fraction one uses scatter plots of the position of secondaries reaching a desired position downstream (e.g. the CDF test area trigger counters). The number of entries in the appropriate area of the scatter plot divided by the total number of simulated events is the desired fraction.

The main advantages of using Anthony Malensek's versions of DECAY are that they allow an absolute yield calculation and that they allow the production and transport of particles other than π's (e.g. protons and positrons).

Using the above method, the yields at MT6 were estimated for a 1"×1" area for π's (table 11), protons (table 12) and positrons (table 13). Note that all these are produced with the primary target only. The momentum spread of the beams is given by the simulations as $\pm 3\%$ for 5 - 227 GeV/c.

In tables 11, 12 and 13, the numbers in column 2 give the number of secondaries of the type requested, with position, angle and momentum in the ranges requested, per interacting primary proton. Column 3 provides the fraction of the secondaries counted in column 2 that will be successfully transported to a 1"×1" area centered on the beam, at MT6.

From the way the numbers in columns 2 and 3 are defined, it can be seen that they depend on the 'BEAM' card parameters in DECAY-TURTLE. Only their product has physics relevance. These numbers are provided solely as guide-posts to the simulation process.

p_{π^+} (GeV/c)	$\pi/p_{\mathrm{interacting}}$	$N^{\mathrm{MT6}}_{\mathrm{inch}^2}$	Yield (π^+/spill)	Input Deck[2]
5	0.000186	146/100000	0.046×10^6	MTPI005.DAT
10	0.000635	299/100000	0.32×10^6	MTPI010.DAT
25	0.00254	444/100000	1.9×10^6	MTPI025.DAT
50	0.00547	261/50000	4.8×10^6	MTPI050.DAT
75	0.00776	258/50000	6.8×10^6	MTPI075.DAT
150	0.0140	294/50000	$14. \times 10^6$	MTPI150.DAT
227	0.0168	324/50000	$18. \times 10^6$	MTPI227.DAT

Table 11: Absolute pion yields in hadron beams

The estimated μ^+ yield (see tables 5 and 6) was obtained by producing histograms of μ^+ positions in the π^+ simulations. The number of entries was then multiplied by the number of interacting primary protons per spill and by the ratio of secondary π^+ to interacting protons and divided by the number of events simulated. This estimate does not take into account μ^+'s produced in nuclear interactions in material (e.g. targets, windows, air, etc.).

[2] Files can be found according to the path: RDIV01::RFD$DISK1:[GANEL.PI96]filename.DAT .

p_p (GeV/c)	$p/p_{interacting}$	$N^{MT6}_{inch^2}$	Yield (p/spill)	Input Deck[3]
5	0.00000438	573/100000	0.42×10^4	MTPR005.DAT
10	0.0000177	572/100000	0.17×10^5	MTPR010.DAT
25	0.000115	556/100000	0.11×10^6	MTPR025.DAT
50	0.000483	524/100000	0.43×10^6	MTPR050.DAT
75	0.00114	507/100000	0.97×10^6	MTPR075.DAT
150	0.00507	550/100000	4.7×10^6	MTPR150.DAT
227	0.0123	590/100000	$12. \times 10^6$	MTPR227.DAT

Table 12: Absolute proton yields in hadron beams

p_{e^+} (GeV/c)	$e^+/p_{interacting}$	$N^{MT6}_{inch^2}$	Yield (e^+/spill)	Input Deck[4]
5	0.0608	48/1000000	0.49×10^4	MTES005.DAT
10	0.0608	102/1000000	1.0×10^6	MTES010.DAT
25	0.0608	214/1000000	2.2×10^5	MTES025.DAT
50	0.0608	299/1000000	3.1×10^6	MTES050.DAT
75	0.0608	259/1000000	2.6×10^6	MTES075.DAT
150	0.0608	145/1000000	1.5×10^6	MTES150.DAT
227	0.0608	70/1000000	0.72×10^6	MTES227.DAT

Table 13: Absolute positron yields in hadron beams

B Positron Beam Yield Calculations

The process is slightly more complicated for positrons. Here, we start out by simulating positrons of 150 GeV/c (or 227 GeV/c) produced at MT2CON2 (or MT2CON1) and transported to MT3CON1. There we change the beam momentum to the low momentum desired, keeping angular and lateral profiles unchanged, and increasing the momentum spread to σ =8%. The lower momentum beam is then transported to MT6. The rates from this procedure are given in table 14.

One should note that the procedure of lowering beam momentum and increasing momentum fluctuations also randomizes the correlation between incidence position of high momentum positrons on MT3CON1 and their momentum. This is actually beneficial, as there is only a very small correlation between the high momentum value and the ratio of low momentum to high momentum rates exiting and entering the radiator, respectively.

p_{e^+} (GeV/c)	$e^+/p_{interacting}$	$N^{MT6}_{inch^2}$	Yield (e^+/spill)	Input Deck[4]
150	0.1010	24/1000000	0.41×10^6	MT150E010.DAT
227	0.0393	261/10000000	0.17×10^6	MT227E010.DAT

Table 14: Low momentum positrons at MT6 (assuming one low momentum positron per high momentum positron with σ_p =8% at MT3CON1)

As the optics are the same for all energies (currents are scaled proportionally to momentum) and there are no decays for electrons (the in-flight decay option was turned off), the rate of low energy positrons successfully

[3] Files can be found according to the path: RDIV01::RFD$DISK1:[GANEL.PI96]filename.DAT .
[4] Files can be found according to the path: RDIV01::RFD$DISK1:[GANEL.ES96]filename.DAT .

transported to MT6 is momentum-independent.

Since the ratio of low momentum positrons exiting MT3CON1 to high momentum positrons incident on MT3CON1 is momentum dependent, EGS4 simulations were used to estimate it (see tables 15 and 16).

p_{out} (GeV/c)	0.25 (X_0)	0.50 (X_0)	0.75 (X_0)	1.00 (X_0)	1.36 (X_0)	1.50 (X_0)	2.00 (X_0)	2.50 (X_0)	3.00 (X_0)	3.50 (X_0)
1.0	0.001	0.003	0.005	0.008	0.013	0.015	0.023	0.033	**0.042**	0.048
5.0	0.007	0.019	0.041	0.058	0.101	0.115	0.151	0.193	**0.203**	0.213
10.0	0.006	0.023	0.042	0.059	0.083	0.095	0.126	0.131	**0.125**	0.116
25.0	0.015	0.028	0.044	0.056	0.072	**0.080**	0.074	0.074	0.053	0.039
50.0	0.021	0.044	0.058	0.068	0.066	**0.063**	0.053	0.034	0.021	0.012
75.0	0.036	0.063	**0.076**	0.078	0.064	0.057	0.035	0.015	0.010	0.004
100.0	0.070	0.103	**0.105**	0.087	0.057	0.041	0.018	0.007	0.002	0.001
125.0	0.156	0.177	0.126	0.081	0.036	0.025	0.005	0.002	0.000	0.000
150.0	0.475	0.192	0.077	0.026	0.005	0.003	0.000	0.000	0.000	0.000

Table 15: Ratios of lower energy positrons to higher energy incident positrons for various radiator thicknesses and out-going energy bins (σ_p =8%). Incident momentum of 150 GeV/c used.

p_{out} (GeV/c)	0.25 (X_0)	0.50 (X_0)	0.75 (X_0)	1.00 (X_0)	1.36 (X_0)	1.50 (X_0)	2.00 (X_0)	2.50 (X_0)	3.00 (X_0)	3.50 (X_0)
1.0	0.001	0.003	0.005	0.008	0.016	0.017	0.030	0.041	0.052	0.063
5.0	0.007	0.018	0.039	0.065	0.105	0.121	0.182	0.230	0.273	0.282
10.0	0.008	0.019	0.039	0.063	0.095	0.104	0.151	0.169	0.176	0.169
25.0	0.009	0.024	0.039	0.060	0.077	0.088	0.099	0.098	0.087	0.070
50.0	0.013	0.028	0.047	0.062	0.072	0.077	0.067	0.053	0.039	0.028
75.0	0.020	0.039	0.055	0.067	0.065	0.070	0.055	0.034	0.020	0.011
100.0	0.034	0.057	0.068	0.072	0.069	0.062	0.040	0.026	0.011	0.006
125.0	0.045	0.070	**0.085**	0.080	0.059	0.052	0.025	0.011	0.006	0.003
150.0	0.066	0.100	**0.100**	0.079	0.053	0.040	0.016	0.007	0.002	0.002

Table 16: Ratios of lower energy positrons to higher energy incident positrons for various radiator thicknesses and out-going energy bins (σ_p =8%). Incident momentum of 227 GeV/c used.

EGS4 shows that the highest ratio of outgoing to incoming positrons for 75 GeV/c incident and 10 GeV/c outgoing is about half the highest ratio for 150 GeV/c and 227 GeV/c incident and 10 GeV/c outgoing - thus the 75 GeV/c option is not considered here.

For the highest momentum positron beams (over 100 GeV/c), it is better to use the 227 GeV/c secondary beam to minimize hadron contamination of the positron beam (the bending magnets from MT3 and on will be tuned far below the currents required to steer 227 GeV/c hadrons to MT6).

Note that each bin has a full width 16% of the listed momentum (e.g. 50 GeV/c is actually 50 GeV/c ± 4 GeV/c), and that each entry (combination of incident momentum and radiator thickness) is based on a run of 10000 events, and provides the ratio of out-going lower-momentum positrons to incident positrons (within 1 mr of the direction of the incident positrons).

Radiator thickness is chosen to maximize the ratio, but some compromises are made to limit the number of radiators to 3 - the target wheel has 4 openings and one must be left empty (see figure 8). The ratios in bold-face indicate the optimal combinations chosen.

When comparing entries in the two tables one should remember that in terms of absolute yields, an entry in

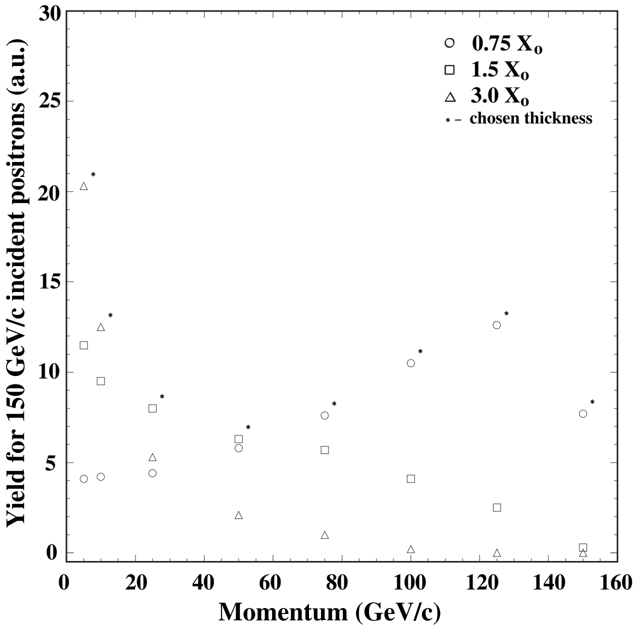

Figure 8: Ratios of outgoing to incident positron fluxes for various radiator thicknesses (EGS4 simulations)

table 16 must exceed the same entry in table 15 by at least 140% to indicate a better choice. The only reason to accept lower yields (as in the case of 125 GeV/c and 150 GeV/c out-going beams) by choosing 227 GeV/c incident positrons is to improve purity.

The EGS4 [3] derived ratio was multiplied by the rates predicted by DECAY to give the best estimate for actual rates at MT6 (see table 17).

p_{low} (GeV/c)	e^+ Yield at MT6 (e^+/spill)
1	17100
5	82300
10	50800
25	32300
50	25400
75	30700
100	42400
125	14500
150	17000

Table 17: Absolute positron yields at the CDF test area per (1.0×10^{12} primary proton) spill

Note that these numbers are much lower than the number of positrons in the secondary hadron beams (for momenta above 10 GeV/c). The reason to use this method is that in the hadron mode, there will be between factor 2 and factor 50 more hadrons and muons than positrons in the beam, which will make the beam unusable for most positron beam applications.

C The MT Čerenkov Counter

The MT Čerenkov counter (MT4CC) is briefly outlined below:

location	between MT4Q2 and MT4SC
dimension	approximately 30 m in length
support	steel
design	Threshold type
Gas	He (refraction index = 1 + 2.6 $\times 10^{-6} \times$ P(PSIG))
Pressure range	0-12 PSIG
High Voltage	2400 V

Table 18: Basic parameters of the Meson Test Čerenkov counter

This detector was decomissioned in the summer of 1996. It is now a vacuum pipe. The upstream pressure window was removed and the ex-Čerenkov counter pipe was coupled to the beam pipe. The gas system, mirror and PMT were removed and stored in the Proton Assembly Building (PAB) at FNAL. The downstream pressure window was converted to a vacuum window.